agronomy

MDPI

Review

An Ongoing Blended Long-Term Vegetation Health Product for Monitoring Global Food Security

Wenze Yang [1,*], Felix Kogan [2] and Wei Guo [1]

[1] I M Systems Group Inc., College Park, MD 20740, USA; Wei.Guo@noaa.gov
[2] Center for Satellite Applications and Research, National Environmental Satellite Data and Information Services (NESDIS), National Oceanic and Atmospheric Administration (NOAA), College Park, MD 20740, USA; Felix.Kogan@noaa.gov
* Correspondence: Wenze.Yang@noaa.gov; Tel.: +1-301-683-3577

Received: 26 October 2020; Accepted: 7 December 2020; Published: 9 December 2020

Abstract: Remotely observing global vegetation from space has endured for nearly 50 years. Many datasets have been developed to monitor vegetation status. Tailored to specifically monitor global food security concerning drought and crop yield, a suite of datasets based on vegetation health concepts and Advanced Very High Resolution Radiometer (AVHRR) observation was developed in the 1980s and utilized throughout the world. Nowadays, satellites based imaging radiometers have evolved into the Visible Infrared Imaging Radiometer Suite (VIIRS) era. With proper algorithm development, the blended version of the data suite, composed of the AVHRR dataset from 1981 to 2012 and VIIRS dataset from 2013 and afterwards, has bridged the long-term AVHRR observation and high-quality VIIRS data. This paper explains the blended version of the data suite.

Keywords: NDVI; vegetation health; AVHRR; VIIRS; long-term; drought; crop yield; food security

1. Introduction

The coincidence of the Great Grain Robbery [1,2] and the launch of LandSat 1 (then by the name of "Earth Resources Technology Satellite (ERTS)", or sometimes together with label "1" or "A") in July 1972 represented the human race entering a new era of agricultural monitoring. The lessons learned from the crisis of the Great Grain Robbery called for the necessity to be aware in advance of agricultural emergencies over a large area or even the globe; it also spurred huge multi-agency projects, such as the Large Area Crop Inventory Experiment (LACIE) in 1974 and the subsequent Agriculture and Resources Inventory Surveys through Aerospace Remote Sensing (AgRISTARS) program in 1978 [3]. The multi-spectral scanner (MSS) observation from LandSat 1 echoed with technological readiness of agricultural monitoring from space to some degree and heralded the future direction: on the one hand, it has been utilized to measure crop area in LACIE [4], as well as to deal with land cover classification, identification of crop type, assessment of crop condition, and so on, in AgRISTARS [5]; on the another hand, it has pioneered successive Earth Observatory, as following LandSat series, Advanced Very High Resolution Radiometer (AVHRR) series, Moderate Resolution Imaging Spectroradiometer (MODIS), SPOT (Satellite Pour l'Observation de la Terre)—VGT, Visible Infrared Imaging Radiometer Suite (VIIRS), etc. Therefore, as can be seen, from the starting point of global agricultural monitoring, product development and applications have been tightly coupled and have stepped forward in an alternating fashion, like two legs of a human being: applications set new and higher requirements to product development; product development provides solutions to applications, and spurs new areas of applications; then, they together enter a higher and wider loop. Many other successful products also follow this development pattern.

Facing the requirement of vegetation applications, and based on MSS data experiences and in situ spectrometer data, Tucker [6] systematically compared 18 types of spectral combinations (half of them between red (0.63–0.69 μm) and near infrared (NIR, 0.75–0.80 μm) bands, and another half between red and green (0.52–0.60 μm) bands) with 16 biophysical characteristics measured from September 1971 to October 1972, and concluded that the linear combinations of the red and NIR radiances "can be employed to monitor the photosynthetically active biomass of plant canopies". This was the beginning of the Normalized Differential Vegetation Index (NDVI).

The AVHRR, first on board the Television and Infrared Observation Satellite (TIROS)–N and NOAA-6 satellites, launched in October 1978 and June 1979, respectively, originally had the spectral configuration of its first channel as 0.55–0.90 μm, roughly spreading from green to NIR, designed for meteorological applications. Then, since the onboard NOAA-7 satellite launched on June 23, 1981, the spectral configuration of its first channel was altered to the upper portion of 0.55–0.70 μm, applicable to derive NDVI, thus enabling the "extensive and widespread AVHRR NDVI works" [7].

Facing the worldwide usage of AVHRR NDVI, Kogan [8] presented interpretative problems of NDVI at different ecosystems, e.g., an NDVI value of 0.3 might be low in a wet ecosystem, but it might already surpass the maximum in a dry ecosystem. Therefore, stratification of the NDVI values was required to assess weather impacts on vegetation in non-homogeneous areas. The stratification resulted in the Vegetation Condition Index (VCI), which could be simply illustrated as

$$\mathrm{VCI} = 100 \times (\mathrm{NDVI} - \mathrm{NDVI}_{min}) / (\mathrm{NDVI}_{max} - \mathrm{NDVI}_{min}), \quad (1)$$

where NDVI_{max}, and NDVI_{min} are the multi-year absolute maximum and minimum of NDVI. As VCI is more sensitive to rainfall dynamics comparing to NDVI, it is a better indicator of vegetation response to precipitation impact [8].

Although VCI is capable of capturing water-related stress, it could be augmented by the introduction of the Temperature Condition Index (TCI), for determining temperature-related vegetation stress and also stress caused by an excessive wetness [9]. TCI is defined as

$$\mathrm{TCI} = 100 \times (BT_{max} - BT) / (BT_{max} - BT_{min}), \quad (2)$$

where BT, BT_{max}, and BT_{min} are the Brightness Temperature, originally derived from AVHRR's fourth channel (10–11.5 μm), its multi-year absolute maximum, and minimum, respectively.

By combining VCI and TCI through weighted averaging, one can obtain the Vegetation Health Index (VHI) as

$$\mathrm{VHI} = \alpha \times \mathrm{VCI} + (1 - \alpha) \times \mathrm{TCI}, \quad (3)$$

where, in a general sense, the weight α is simply 0.5.

By definition, the values of the three indices range from 0 to 100, indicating most stressed (0) to most favorable (100). The value range of 35 to 65 generally indicates normal condition.

Based on Equations (1)–(3), the vegetation health product (VHP, including VCI, TCI and VHI) has been developed and utilized to address global food security problems (food security problems include availability of food, access to food, utilization of food, stability, and malnutrition; drought and crop yield estimation are major sub-problems of availability of food and stability) since its early stage, mainly based on the two features: its capacity to detecting and tracking drought, and its readiness to estimating crop yield prior to harvest.

The direct application of vegetation health product on drought has been documented throughout the world, e.g., to measure drought's onset time, intensity, duration, and impact on vegetation in the United States [9–11], Southern Africa [12], China [13], India [14], Mongolia [15], and elsewhere [16]. Furthermore, VHI has been selected as one of six key objective drought indicators (the other five selected indicators are Palmer Drought Severity Index (PDSI), Soil Moisture from Climate Prediction Center (CPC/SM), United States Geological Survey (USGS) daily streamflow percentiles, percent of

normal precipitation, and Standardized Precipitation Index (SPI)) to be used by the U.S. Drought Monitor (USDM) [17]. It is worth mentioning that in the World Meteorological Organization (WMO) workshop focusing on agricultural drought, held in June 2010 in Murcia, Spain [18], although a consensus recommendation on a single index had not been reached, one plausible conclusion was that a composite index, as USDM, should be considered to characterize agricultural droughts. Note also that the national scale USDM has been extended to continent scale in the North American Drought Monitor (NADM) [19], and would perform as the backbone in the Global Drought Monitor (GDM) [20,21], so that VHI would contribute to monitoring drought indirectly through these magnificent systems.

In mainstream crop yield modeling, agricultural technology (which may also include agricultural policy, fertilizer usage, and other non-weather factors) and weather are two major factors to impact crop yield [22,23]. The former could be modeled as a long-term trend, and the latter as the departure from the trend. As the vegetation health product captures water-related and temperature-related response of crops, it is a good indicator of crop growth, and therefore is a good indicator of crop yield due to weather impacts. To date, the vegetation health product has been widely used in modeling or estimating many kinds of crop yield in many countries or regions; Table 1 presents some examples of these applications.

Table 1. Applications to utilize vegetation health product for estimating crop yield.

	Crop	Wheat	Corn	Rice	Soybean	Potato
Global	[24,25]					
US	[26]	[27,28]	[29]			
Ukraine	[30]	[31,32]				
Argentina	[33–35]					
Bangladesh				[36,37]		[38,39]
Brazil					[40]	
Poland	[41]					
Kazakhstan	[42]					
India	[43]					
Russia	[44]					
Australia		[23]				
China			[45]			
Southern Africa			[46]			

As the vegetation health product may perform as indictor for both drought and crop yield, it has been considered to serve as backbone in the framework of index-based agricultural insurance [42,47]. Compared to traditional indemnity based instruments, the index-based insurance is more objective and exogenous; after proper designing, it would automatically trigger the payouts for insurance contracts without tedious field assessments, which would reduce administrative costs, so as to lower the premiums, as well as timely payouts.

Note that the vegetation health concept was born in the AVHRR era, and a considerable amount of relative vegetation health product applications were conducted using an AVHRR-based product. After the introduction of VIIRS in 2013, and coexistence of both AVHRR-based and VIIRS-based product from 2013 to 2017, the operational processing of NOAA AVHRR for the vegetation health product has ceased since the end of 2017. How will the relatively new VIIRS-based vegetation health product inherit the long-term AVHRR's legacy? How can the users be enabled avoid the jump from the AVHRR era to the VIIRS era? This article focuses on elucidating answers to these questions.

The organization of this article is as follows: the materials and methods are presented in Section 2; product development in the AVHRR and VIIRS era is reviewed in Sections 3 and 4; recent applications on drought and crop yield are reviewed in Sections 5 and 6; discussion focusing on product development of the blended AVHRR/VIIRS product is given in Section 7; and conclusions focusing on its applications are provided in Section 8.

2. Materials and Methods

Although a number of vegetation health products have been developed based on the vegetation health Equations (1)–(3), such as the ones derived from the MODIS [48,49] and Landsat data [50,51], the VHP reviewed in this article is confined to the vegetation health products developed in Center for Satellite Applications and Research, National Environmental Satellite Data and Information Services, NOAA, and its URL is https://www.star.nesdis.noaa.gov/smcd/emb/vci/VH/index.php.

The blended VHP is composed of AVHRR VHP (1981–2012) and VIIRS VHP (2013 onward). It can be regarded as an extension of the long-term AVHRR product with high-quality VIIRS observations.

Like all other datasets, a complete product development of the blended VHP includes algorithm development and validation. Due to the blended nature of the product, the product development could be clearly divided into different periods, as the AVHRR era and the VIIRS era.

The essential elements in algorithm development, as indicated in Equations (1)–(3), are NDVI/BT, their climatology, and the weight α. The prime algorithm development activities in the AVHRR era related to improving the quality of NDVI, while in the first stage of the VIIRS era, due to much higher quality of VIIRS NDVI, more attention was paid to their climatology. In the next stage of the VIIRS era, the focus could be the weight α.

As direct validation of VHP is nearly impossible, two sorts of indirect validation approaches have been used: 1. comparison with indirect indicators, which has been widely used in the AVHRR era; and 2. comparison with previous products, more widely used in the VIIRS era.

Indirect indicators could be agricultural, economic, and human health data, e.g., higher VHI values could correspond to higher crop yield, as indicated in Section 1. In this sense, some validation works mingle with the VHP application.

This article reviews how the blended VHP came into being, and projects some future directions. Most of the materials of this review were from published works, in order to fill some potential gaps; especially due to the relatively short span of the VIIRS era, some formerly unpublished materials were also utilized.

3. Review of Product Development in the AVHRR Era

Within the usage of VHP, the AVHRR has on-boarded a series of NOAA satellites: NOAA-7, -9, -11, -14, -16, -18, and -19. The early stage of AVHRR era was featured with noise characterization and removal from the remotely observed data, which have been addressed in the product development of Global Inventory Monitoring and Modeling Studies (GIMMS) [7,52] and Pathfinder Advanced Very High Resolution Radiometer Land (PAL) [53], and their applications in research [54,55]. Although the major products of VHP are VCI, TCI, and VHI, considerable efforts had been put on noise correction of lower level products: NDVI and BT.

There are a number of sources where noise would be brought to satellite data, including physical, geometrical, mechanical, mapping, environmental, or of random origin. They could impact on a variety of dimensions: long- or short-term, increasing or decreasing the values, the varying amplitude being large or small, systematic or random, etc.

Within a series of noises, VHP identified following most important ones: (1) contamination of cloud and aerosol, which would greatly reduce the value of NDVI and BT; (2) sensor degradation and orbital drift, which would make the measurement of a sensor vary from start of its launch to later stages; (3) the eruption of El Chichon volcano in Mexico in April 1982, and the eruption of Mt Pinatubo volcano in the Philippines in mid-June 1991, which made high aerosol loading in surrounding air flow, and thus decreasing NDVI and BT; (4) the visible band has been narrowed to avoid Oxygen and part of Ozone absorption from AVHRR-2 to AVHRR-3, which would make AVHRR-3 NDVI higher than AVHRR-2 NDVI; (5) other high frequency noise aroused from residual of cloud clearing, atmospheric transparency, surface anisotropy, data processing, etc., which would generate erratic NDVI and BT values.

Accordingly, considering the cumulative response of vegetation towards the surrounding environment, weekly change could be sufficient to capture the phenology; thus, all global vegetation datasets have a temporal resolution of weekly or lower (8-day, half monthly, etc.). VHP adapted the greatest NDVI value within a week to remove cloud and aerosol. To account for sensor degradation, orbital drift, and volcanic eruption, firstly, VHP kept using most updating post-launch coefficients to generate NDVI and BT; secondly, based on the assumption that for large areas, the NDVI reduction due to technical and external forces (orbital drift, volcanic eruptions, etc.) is larger than the weather-related NDVI changes from year to year, the Empirical Distribution Function (EDF) method was applied to impacted latitude zones and periods; thirdly, if the local equator crossing time (LECT) of one satellite (Sat A) had been later than 3 pm, and there was another substitute satellite (Sat B), then data from Sat A would be replaced by data from Sat B. Based on statistical calculation, compensations were made to NDVI generated from NOAA-16 to -19, and NOAA-7 to -9, to decrease the discrepancy between AVHRR-2 to AVHRR3. Lastly, the median filter was applied to remove high frequency noise from sorts of sources, thus the generation of a set of smoothed NDVI (SMN) and BT (SMT). More details on this aspect could be referred to [22,56] and the references in them.

From the perspective of product data flow, the starting point of vegetation health product is the smoothed NDVI/BT: SMN and SMT. First, the climatology is built upon SMN and SMT. Second, VCI, TCI and VHI are calculated upon SMN and SMT. In the AVHRR era, the prevailing spatial resolutions of the datasets are 16 km and 4 km, suitable for large scale application.

The direct validation of VCI/TCI/VHI is nearly impossible, as these values are not directly observable due to the introduction of historical smoothed NDVI and BT values. Then, indirect validation was adopted as the solution to this problem, which generally falls into two approaches: comparison with indirect indicators, and comparison with previous products.

Fortunately, one such indirect indicator could be the quantification of drought—e.g., onset time, intensity, duration, and impact on vegetation, economic impacts—in the regions where water availability and temperature serving as limiting factors to vegetation growth, crop yield could be another such indirect indicator. Therefore, the drought and crop yield related applications listed in Section 1, from another aspect, could be regarded as validation works of VHP.

The second indirect validation approach, comparison with previous products, would be more widely used in the VIIRS era, which will be demonstrated in Section 4.

One important task in the AVHRR era was the building of climatology. Featured with extreme values, maximum and minimum, the climatology could be evolving with time: in a year, if a place experienced severe drought, its minimum NDVI could get lower; in a year, if a place encountered heat wave, its maximum BT could get higher; in the areas with land use, land change (desertification, forestation, deforestation, etc.), there would be emerging greens and browns, which might be translated to new maximum and/or minimum; there could be vegetation responses to climate change in high altitudes or high latitudes; etc. All these updates are imperative to integrate into the climatology. Thus, with accumulation, a long-term climatology could be dramatically different from its short-term version [57]. Recorded as historical values, the numbers integrated into climatology have more strict criteria than common SMN and SMT products to further avoid extraneous noise; for example, in the years 1988, 1993 and 1994, although the time series of SMN and SMT continued, the records were excluded from the climatology due to relatively lower quality. Although not well documented and/or published, in the AVHRR era of 1981–2017, the AVHRR climatology was updated a number of times, and the consecutive VCI/TCI/VHI had been reprocessed accordingly.

4. Review of Product Development in the VIIRS Era

Currently, VIIRS has been on-board the Suomi National Polar-orbiting Partnership (S-NPP) and Joint Polar Satellite System (JPSS)-1 (renamed to NOAA-20 after launch); the next on-board satellites, JPSS-2, -3, and -4, are scheduled in 2021, 2026, and 2031, respectively [58], and their observations are expected to continue for the next two more decades.

As the successor to AVHRR and MODIS, and the first on-board satellite (S-NPP, launched in 2011, 30 years after the launch of NOAA-7 in 1981), VIIRS has displayed overwhelming improvements for Earth observation and monitoring global food security: wider swath, a sharper view of the swath edge, multiple spectral channels, higher spatial resolution, narrower response function, excellent radiometric features, faster data processing, higher data accuracy, etc. [59]. It is worth emphasizing that the inclination angle of VIIRS on-board satellites have been periodically adjusted to maintain their equator crossing time around the designed value [60], so VIIRS experiences minimal drift. Further, due to no mega scale volcano eruption (such as El Chichon or Mt Pinatubo) yet in the VIIRS era, much fewer efforts are needed for noise correction of lower level products, compared to those in the AVHRR era.

In order to extend the decadal efforts from the AVHRR era, the principle question is how to continue AVHRR data records using VIIRS observations: achieving data continuity at SMN/SMT level, or at VCI/TCI/VHI level.

The first such attempt was made in 2015 [61]. Considering VIIRS SMN/SMT values are different from those of AVHRR, mainly due to VIIRS's narrower response function, ref. [61] converted VIIRS values to AVHRR values using linear regressions, and made use of AVHRR climatology to calculate VCI and TCI. The linear regression performs good at intermediate values, but is poor at extreme values, so this approach fails to capture the dynamic value range, and thus produces erroneous VCI/TCI distribution.

Noting that the biggest disadvantage of VIIRS data is its short duration, a second attempt was made in 2018 [57]. Instead of converting SMN/SMT values, [57] extended the VIIRS short-term climatology into a pseudo long-term climatology. With the assumption that "the same N years of contribution to climatology is the same between VIIRS and AVHRR", [57] derived a simple equation to express the pseudo VIIRS 36-year climatology using the AVHRR 36-year climatology and their overlapping 5 year climatology. As a result, the second generation of VIIRS VCI/TCI/VHI reaches the continuity, it could trace the signature of the long-term AVHRR vegetation health products closely, in terms of histogram, correlation coefficients, time series, and so on, which expedites the maturity of the VIIRS VHP by more than one decade.

A step further, [62] re-interpreted Equation (1) as de-compositing NDVI into VCI and its climatology. By theorizing VCI as vegetation carrying capacity, this capacity should be similar from different sensor observations, and sensor-specific information mostly is mostly stored in their climatology, [62] inversely used this equation for re-compositing cross-satellite/cross-product NDVI from VCI and their distinctive climatology. The re-composited NDVI agrees well with the original NDVI spatially and temporally, with an accuracy of 0.02 NDVI unit at a global scale. This technique can be naturally applied to BT by inversely using Equation (2), which enables the possibility to convert the long-term AVHRR NDVI/BT into VIIRS scale, or keep on generating AVHRR scale NDVI/BT using VIIRS observation. In a word, the continuity at SMN/SMT level has been realized.

The blended data are thus combined from AVHRR and VIIRS. Figure 1 compares the blended SMN and SMT time series from mid-1981 to the end of 2019 with regards to the benchmark values in the AVHRR era: note the data since 2013 are actually observations from VIIRS using the re-compositing approach [62]. The benchmark values are weekly averages according to each latitudinal band, from following 5 years of smoothed values: 1989, 1990, and 1995–1997, which are regarded as the best quality observation years of AVHRR [22]. It is clear that, in the benchmark years, both the difference of NDVI and BT are very low. Although specific corrections were applied to the data, there still remain residual errors several years after 1982 and 1991, which are due to a volcano eruption; residual errors occurred also in the periods shortly prior to week 20 of 1995 and the end of 2000, which are mainly due to orbital drift and sensor degradation; in most of the areas, the correction results are in a reasonable range. There are no exceptional errors after 2013, which indicates that the algorithms in [57,62] are effective.

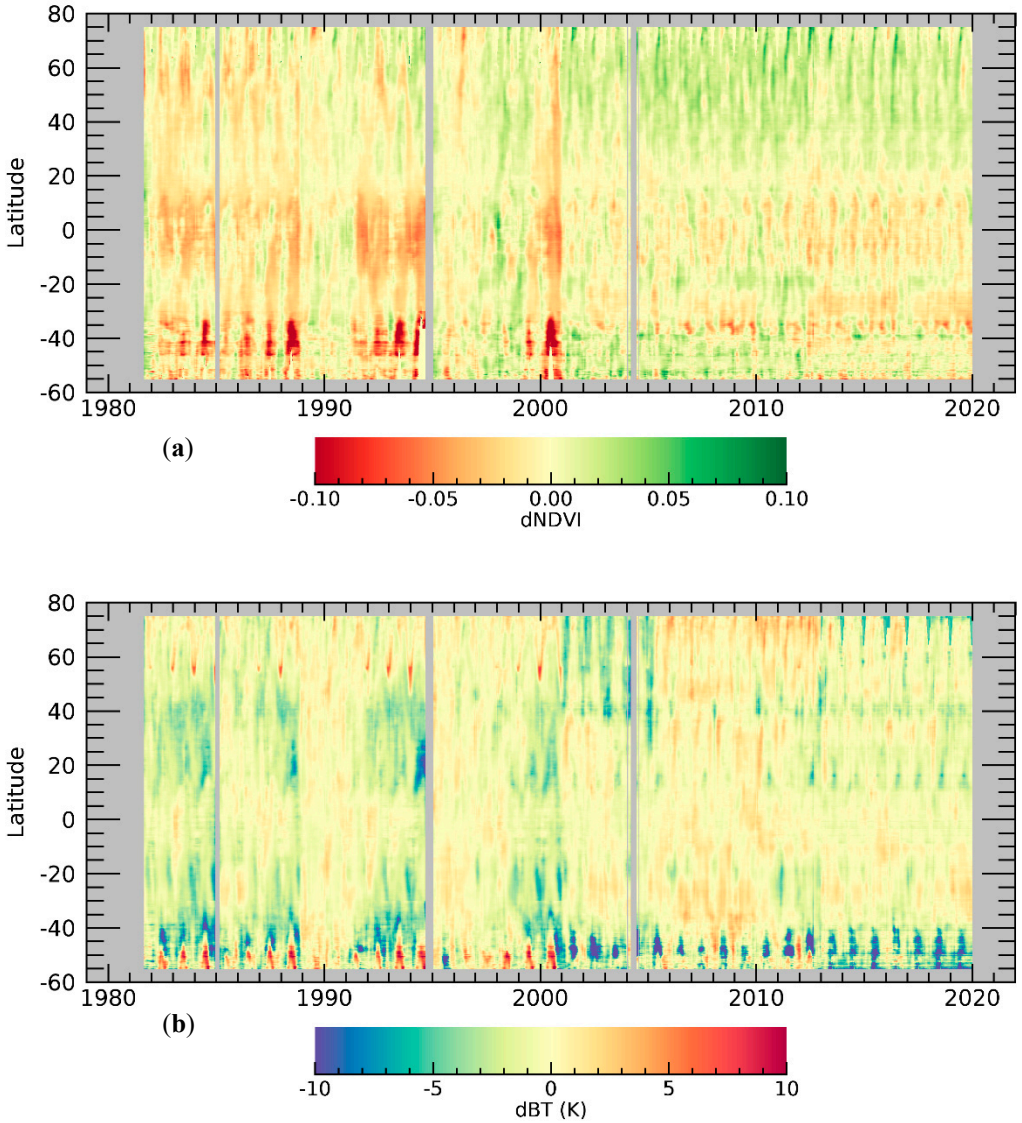

Figure 1. Zonal (4 km resolution) difference between smoothed (**a**) Normalized Differential Vegetation Index (NDVI), (**b**) Brightness Temperature (BT) products and their averaged values from benchmark years: 1989, 1990, and 1995–1997, when there were no serious volcanoes, and other noises were least contaminated. The striking bars indicate data missing in years 1985, 1994–1995, and 2004. Note data from 1981 to 2012 are derived from Advanced Very High Resolution Radiometer (AVHRR), and 2013 to 2019 data are from Visible Infrared Imaging Radiometer Suite (VIIRS). Vegetated land pixels cover from south 55 to north 75, and in each week, valid values in the same latitude are averaged.

In the VIIRS era, the second indirect validation approach, comparison with previous products, has been more widely used. Figure 2 shows the global comparison of weekly VCI derived from S-NPP VIIRS against VCI derived from NOAA-19 AVHRR. Except for some desert areas, only random difference with low amplitude appears. In the desert areas, such as the Sahara desert and Arabian desert, as the multi-year maximum NDVI and minimum NDVI are very low and close, a tiny discrepancy of NDVI between VIIRS and AVHRR would lead to large discrepancy of VCI. Oppositely, in the areas with dense canopy or with distinctive inter-annual vegetation variation, their VCI discrepancy is extremely low.

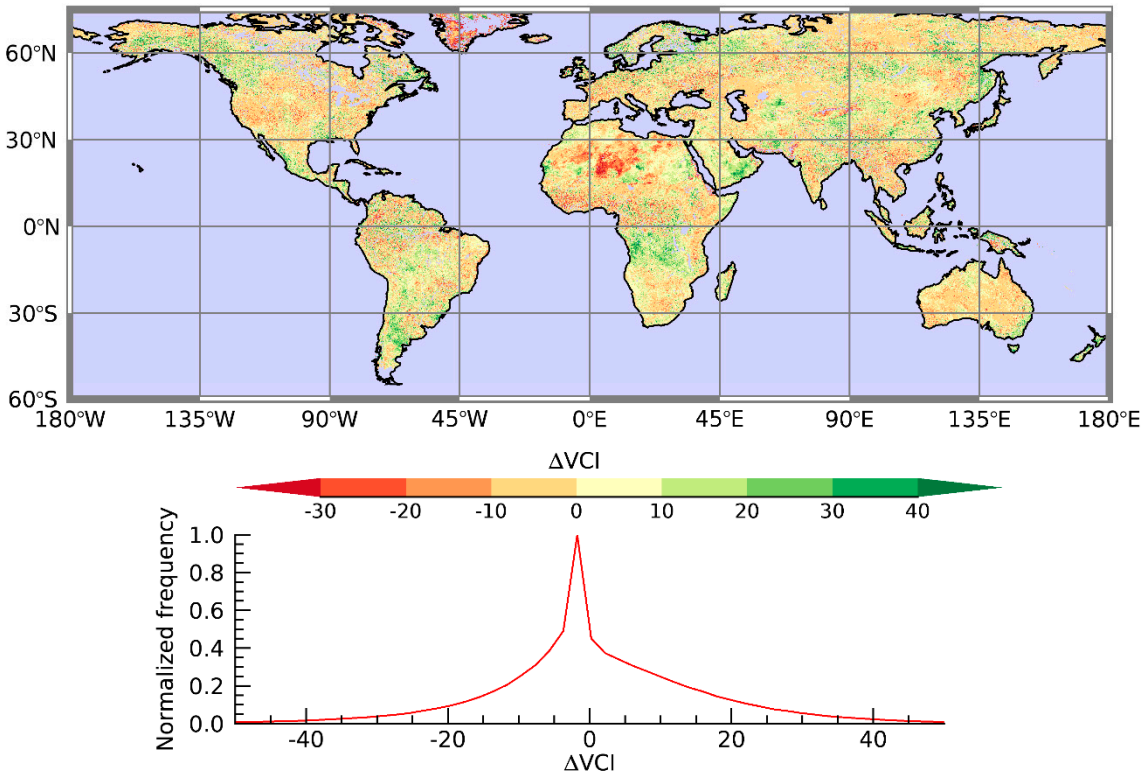

Figure 2. Pixel-level (4 km resolution) difference between Visible Infrared Imaging Radiometer Suite (VIIRS) Vegetation Condition Index (VCI) and Advanced Very High Resolution Radiometer (AVHRR) VCI derived during the period Week 30 (23–29 July), 2016 and its histogram.

Similarly, the product suite (including reflectance at channel 1 (I1) and channel 2 (I2), brightness temperature at channel 5 (I5), NDVI, SMN, SMT, VCI, TCI, and VHI at weekly interval) derived from NOAA-20 VIIRS has been routinely compared against those from S-NPP VIIRS. As expected, after a short period of time after launch, NOAA-20 product suite time series agree very well with S-NPP. In the future, after the launch of JPSS-2, -3, and -4, their product suites are expected to be monitored against S-NPP or NOAA-20.

VIIRS VHP could have wider applications than AVHRR VHP. The prevailing spatial resolutions of the datasets in the AVHRR era are 16 km and 4 km, suitable for applications at continent or country level; in the VIIRS era, the prevailing resolutions are 1 km and 500 m, suitable at province or county level. From one side, more features could be extracted from finer resolution VIIRS products; from another side, VIIRS VHP could be downgraded to coarser resolution, to continue all applications from AVHRR VHP.

The building of climatology remains an important task in the VIIRS era. Although the current VIIRS was built upon a pseudo climatology [57], it mainly covers the moisture and temperature change from 1981 to 2017. With the future climate change, land use, land change and other possible change, new maximum and minimum will definitely appear from the smoothed NDVI and BT datasets, and when necessary, the whole VIIRS climatology would be updated.

5. Recent Applications on Drought

With the introduction of a more advanced sensor, VIIRS, the recent application of the blended VHP on drought goes deeper and wider.

California endured a mega drought from 2006 to 2017. In the peak year of 2012–2015, its area of stronger than moderate vegetation stress reached 70% [63,64]. The drought severely reduced California's surface and ground water by 52% and 28% capacity, respectively. The estimated total

economic drought impact was 2.74 billion USD. However, due to the irrigation system being widely used in California's agricultural area, especially in the Central Valley, the loss in crop revenue was only 3%. Even at the highest peak of the drought period, the 500 m resolution VIIRS VHP could still detect favorable conditions for vegetation. As shown in Figure 3, the blue areas in the middle of California almost delineate the profile of the Central Valley. These are typical irrigation areas. In other irrigation areas, even though the favorable condition was not achieved, their VHI values were still significantly higher than non-irrigation areas, signaling that the impact of the mega-drought had been mitigated in these areas. This feature is absent from the coarser resolution USDM map, and even the 4 km resolution VHP map [64]. However, due to the overdraft of surface and groundwater for irrigation, the deficit of the water level requires more years to recover.

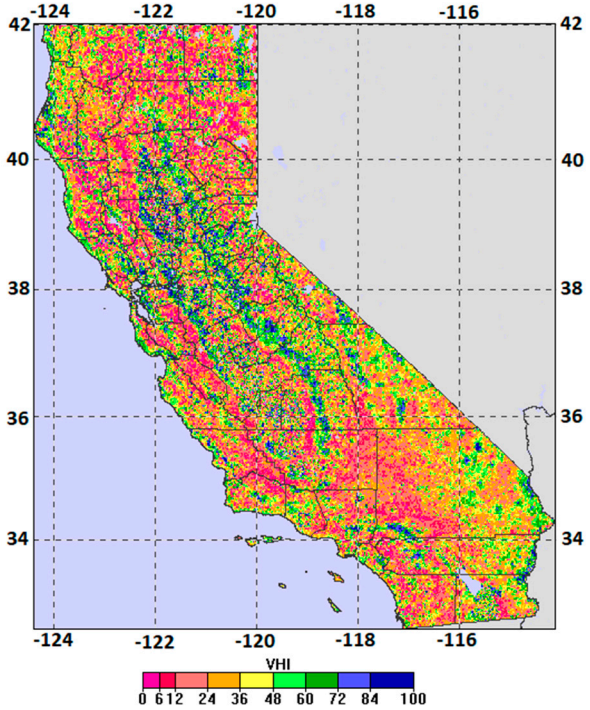

Figure 3. California's Vegetation Health Index (VHI) geographical distribution from 500 m Suomi National Polar-orbiting Partnership (SNPP)/ Visible Infrared Imaging Radiometer Suite (VIIRS) in the period Week 31 (30 July–5 August), 2014.

Texas' 2011 drought featured reduced precipitation from its 40% long-term average, and the agricultural losses were estimated as totaling 7.6 billion USD. Research [65] was conducted on this drought using the then-new satellite Gravity Recovery and Climate Experiment (GRACE), which measures changes in the Earth's gravity field attributed to its surface mass change, mainly attribute to total water storage (TWS) change. On land, TWS accounts for the sum of all groundwater, soil moisture, surface water, snow and ice; thus, it is frequently used in hydrological and cryospherical research. In order to show the exceptional status of the 2011 drought, [65] extended the TWS anomalies time series from January 2003 to September 2012, together with PDSI and precipitation anomalies (in Figure 2 of [65]). Comparably, with the mask of the state of Texas, Figure 4 repeats the time series of the same period, but using VCI, TCI, and VHI. As expected, VHI resembles exceptionally well the fluctuation of the TWS anomaly curve, and VCI follows the precipitation anomaly curve. Besides the exceptional drought of 2011, moderate droughts and water deficits in 2006, 2009, and 2012 were also detected. Furthermore, following TCI time series shown in Figure 4, in several months of 2011, the temperature of Texas hovered and approached its multi-decadal maximum (TCI value close to 0). Compared to the lowest VCI value of ~15, the TCI values of less than 5 suggest that heat waves

contributed more to the magnitude and damage of the drought. Therefore, the 2011 drought of Texas could be regarded as a concurrent drought [66], due to both the precipitation and temperature extreme.

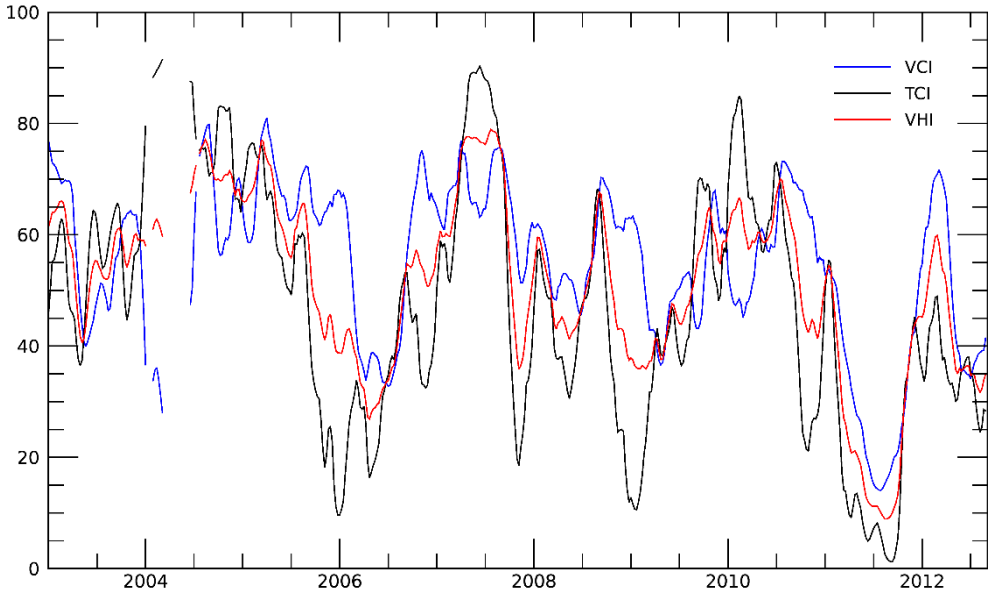

Figure 4. Vegetation health time series of Texas from January 2003 to September 2012, stressing the 2011 drought in this state.

With the background of global warming, and the recognition that on average, droughts can reduce national cereal production by 9–10% [67], it is vital to investigate the trend of droughts in the last few decades. The question of how droughts change with the global warming has turned into to a fierce debate, one mainly based on self-calibrated PDSI: [68] stated drought is increasing due to "decreased precipitation and/or increased evaporation", while [69] concluded "there has been little change in drought over the past 60 years" using variations of PDSI. As a result, Ref. [70] argued that the conflict may arise from how the evapotranspiration component was treated. Using the multi-decadal blended VHP, Ref. [71] characterized the drought dynamic globally, and compared that with the temperature anomaly. The research concluded that the global drought has not intensified, nor expanded; especially, the drought areas may decrease in the major grain-growing countries: China, USA, and India. This conclusion is strongly supported by other independent researches [72,73], indicating human land-use practices, including fertilizer utilization and irrigation, may improve the environmental conditions for crops and/or forests, thus ameliorating food security and mitigating drought.

6. Recent Applications on Crop Yield

Compared to drought application, the calculation of crop yield imposes much more rigorous requirements upon VHP, regarding its phase and magnitude of the time series. As VCI/TCI is by far more sensitive to surface moisture/temperature than NDVI/BT, it is essential to reserve the continuity of VCI/TCI to make VIIRS VHP applicable to crop yield calculation.

To attest the readiness of VIIRS VHP for crop yield application, a continuity check of the time series was performed, accompanying the preparation of [23]. This check was carried out systematically, following the following steps: firstly, land areas on which to grow wheat were identified in five Australian regions: Western Australia, South Australia, Victoria, New South Wales, and Queensland; secondly, the time series were extracted and averaged from these wheat lands, using AVHRR VHP from NOAA-19 and two versions of VIIRS VHP from S-NPP: VIIRS old [61], and VIIRS new [57], during the overlapping years between AVHRR and VIIRS: early 2013 to mid- 2017; thirdly, the different versions of VHP were compared with Australian wheat yield data of corresponding years.

The VHP time series from different sensors/versions is shown in Figure 5. Prior to 2017, when the LECT of NOAA-19 ascending orbit was before 3 pm, AVHRR VHP curves could roughly serve as criteria to judge which version of VIIRS VHP shows more agreement. Clearly, the old version of VIIRS VHP failed to keep accordant with AVHRR, either being frequently out of phase or the magnitude not being quite right. The main reason for this discordance is that AVHRR climatology cannot envelop the converted VIIRS SMN/SMT values, as mentioned in Section 4. Then, we focused on the comparison between the new version of VIIRS VHP and AVHRR. Comparably, the new version of VIIRS VCI followed AVHRR VCI quite well, yet there could be a systematic error between VIIRS TCI and AVHRR TCI: before 2015, the new version of VIIRS TCI was always higher than AVHRR TCI; they reached a good level of agreement during 2015; and then, VIIRS TCI was always lower than AVHRR TCI from 2016.

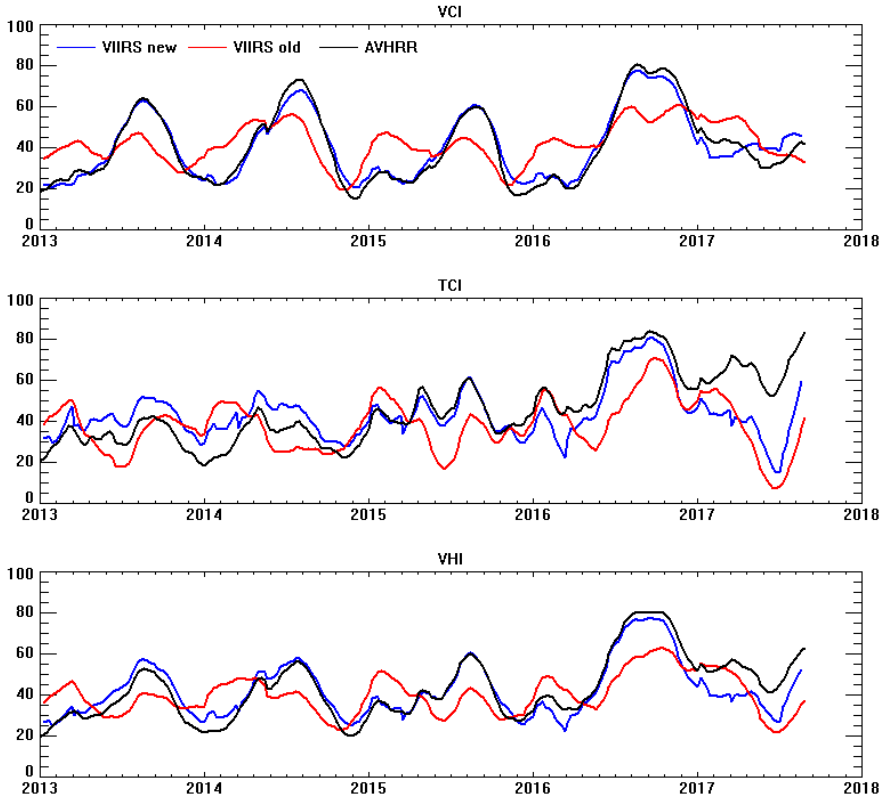

Figure 5. Vegetation health time series of Australian, averaged from five wheat regions weighted by their corresponding areas, from January 2003 to September 2017.

Noting that TCI and BT are inversely related—whenever TCI goes higher, BT goes lower, as indicated in Equation (2)—we can further trace the TCI systematic errors to their relative LECTs. As S-NPP has a controlled orbit, its LECT was fixed around 13:30, while NOAA-19 has varying LECT and kept postponing from 13:35 on 1 January 2013, to 15:30 on 30 September 2017. Combined with other factors, their BT results achieved the best agreement during 2015. Even in 2016, although LECT of NOAA-19 kept delaying, their difference was still within an acceptable range; however, in 2017, NOAA-19 BT went much lower, due to the quite late observing time (appearing as much higher AVHRR TCI values), and as a result, we had to stop AVHRR VHP. In this regard, during the period approaching and after 2017, the new version of VIIRS VHP was more reliable. Therefore, in the blended products, VIIRS data started from 2013.

After confirmation of the continuity with time series, the comparison of various versions of VHI with Australian wheat yield data is still needed to verify their applicability. Following the separation of non-weather trends and weather-related variability (dY), VHI could regress with dY, as shown in

Figure 6. As reported in [23], using AVHRR VHI alone, the correlation coefficient could be greater than 0.77 at the maximum, which is good enough for crop yield application. Considering all the scattered points of AVHRR VHI-dY as a cluster, this cluster could be along the regression line and relatively narrow. By adding two years of the VIIRS old VHI-dY, one can see that one point is at the edge of the cluster, and another point is out of the cluster, which degrades the former correlation coefficient and greatly alters the regression coefficients. However, if we add two years of the VIIRS new VHI-dY, they locate well within the cluster, which regain the former correlation coefficient and the regression coefficients. Adding more years of the new version of VIIRS VHI-dY, the relationship remains the same.

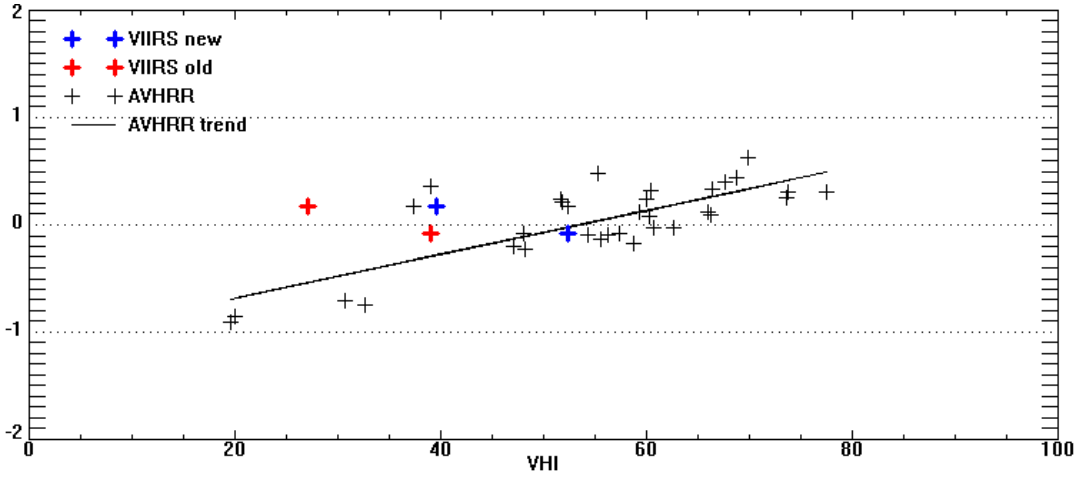

Figure 6. Scatter plots and regression of hard wheat dY versus weekly Vegetation Health Index (VHI) during crop's critical period in Australia.

Similar comparisons have also been carried out at other crop sites or countries, reaching similar results, so the new version of VIIRS VHP could relay the application task in AVHRR's absence.

7. Discussion

Every object has a history which shows its evolution and development, including the blended vegetation health product. The longer we look into its past, the further we can see into its future. Through a long enough timeline, it can be revealed that various aspects have been emphasized at different stages.

Deeply rooted in a real call for agricultural monitoring over a large area and the advancing technology of satellites and instruments, NDVI came into being. Based on NDVI and the surrogate surface temperature, the VHP was established mainly through the Equations (1)–(3). In addition, the product development is tightly related to the items in these equations.

In the early stage, efforts had to focus on improving the quality of the observing items, e.g., NDVI and BT, in the Equations (1) and (2). As there are multiple origins of noise in the satellite products, and noise from different sources may entangle with one another, it is nearly impossible to erase all of the noise source by source, and claim that there is no residual noise in the products. An alternative method is to set an acceptance threshold through solid validation work.

Fortunately, many noise issues have been solved by the new generation instrument VIIRS and its on-board satellites; therefore, in the current stage, product development efforts have shifted to climatology, e.g., $NDVI_{max}$, and $NDVI_{min}$ in Equation (1), and BT_{max}, and BT_{min} in Equation (2). With deepened understanding of the product development, we realized that a climatology with high quality and long-term temporal coverage is essential in order to build an applicable and cross-sensor VHP. In addition, the VIIRS climatology is required to keep updating when necessary.

Through time, critics of VHP might appear in the community. Karnieli et al. [74] argued that in high latitude areas, such as Mongolia, higher temperature implies more favorable temperature

conditions, and thus, this should increase the value of VHI in such regions. Further, [75,76] pointed out that the roles of VCI and TCI are different in assessing drought in different climate regions; therefore, caution should be taken when directly using VHI for this purpose. These arguments are actually closely relevant to the weighting item, α, in Equation (3). Currently, this weighting item is fixed at 0.5 for convenience. In the first publication of TCI and VHI [9], this coefficient was set as 0.7, specifically for the United States. In the future, more research on this could be conducted; the coefficient could be identified in a more systematic way and this could serve as a potential product update.

Product development is not a one-time or static effort; it evolves with changing requirements, and should always be on the way to support relative sorts of applications.

8. Conclusions

Looking back to the Great Grain Robbery in 1972, after nearly five decades, we are now aware both more correctly and further in advance of the possibility of agricultural emergencies of a large area, mainly through modern agricultural monitoring using satellite and information distribution using information and communication technologies (ICTs) [77,78]. Human society can mitigate food security to some extent through ICTs, by macro means as monitoring and early warning, providing timely information regarding potential disasters to governments, improving the food supply chain, and maintaining sustainable agriculture [78], together with many micro means as improving rural households' agricultural production, farm profitability, job opportunities, adoption of healthier practices, and risk management [79].

Drought and crop yield are two important aspects to address global food security: drought measures the loss of food in the impacted temporal–spatial domain, and crop yield measures the productivity of unit crop area. Due to the huge impacts that global food security could incur, providing timely and accurate drought and crop yield information is an imperative requirement for the VHP data suite. As demonstrated in recent applications on drought and crop yield, these applications have been naturally extended into the VIIRS era using the blended product.

To obtain knowledge of a deeper and more comprehensive trend of global drought, further investigations are required in a few more countries, over a longer time period, and attention should also be paid to address more basic issues, such as partitioning the natural and artificial response of drought trends, identifying the role of land use land change to meet the growing food demand during the past decades, sustaining the changing climate, and searching for potential structural change of crops. Predicting crop yield in more countries and for more types of grain is also necessary in order to validate the applicability of the blended VHP. Potentially, this dataset could be used to detect the favorable habitats for desert locust [80,81], adding more dimensions to contribute to food security.

In addition to USDM, currently, the vegetation health product has been used by a number of institutes, agencies, and organizations, including institutes in NOAA, such as Climate Prediction Center (CPC), Climate Diagnostics Center (CDC), National Integrated Drought Information System (NIDIS); departments and agencies in the United States, such as US Department of Agriculture (USDA), US Agency for International Development (USAID), and the Federal Emergency Management Agency (FEMA), in addition to organizations in the United Nations or from around the world, such as the United Nations Food and Agricultural Organization (FAO), the United Nations Educational, Scientific and Cultural Organization (UNESCO), World Meteorological Organization (WMO), and World Health Organization (WHO), etc. This product continues to contribute to the research community, as well as having much broader benefits to human life.

In summary, with proper product development in the VIIRS era, a VHP data series featured with non-jump and non-interrupt characteristics has been created. The blended product bridges the long-term AVHRR observation and high-quality VIIRS data. The applications of the data suite could be continued and possibly expanded. Ongoing research arising from user feedback will surely further improve the quality of the data suite.

Author Contributions: W.Y. was the primary author and all authors contributed to the final paper. F.K. contributed to set and discuss the ideas for this research and helped in all steps of the development of the manuscript. W.G. contributed to discuss the ideas for this research and provided all necessary scientific and technical supports. All authors have read and agreed to the published version of the manuscript.

Funding: This work was funded by JPSS project from National Oceanic and Atmospheric Administration (T2 Y1 WA1 JPSS VIIRS VH).

Acknowledgments: Three anonymous reviewers are thanked for their constructive comments and suggestions. The manuscript contents are solely the opinions of the authors and do not constitute a statement of policy, decision, or position on behalf of NOAA or the U.S. Government.

Conflicts of Interest: The authors declare no conflict of interest.

References

1. Weir, G.E. The Great Grain Robbery: Lessons Learned from Earth Imaging's Early History. 2011. Available online: https://eijournal.com/print/column/defense-watch/the-great-grain-robbery-lessons-learned-from-earth-imaging%E2%80%99s-early-history (accessed on 31 March 2020).
2. Schnittker, J.A. The 1972-73 food price spiral. *Brook. Pap. Econ. Act.* **1973**, *2*, 498–507. [CrossRef]
3. Kosuth, P. Food Security through Earth Observation. 2011. Available online: https://spacenews.com/food-security-through-earth-observation/ (accessed on 31 March 2020).
4. MacDonald, R.B.; Hall, F.G.; Erb, R.B. The use of Landsat data in a large area crop inventory experiment (LACIE). *LARS Symp.* **1975**, *1*, 46.
5. NASA Annual Report. AgRISTARS: Agriculture and Resources Inventory Surveys through Aerospace Remote Sensing. 1981. Available online: https://ntrs.nasa.gov/search.jsp?R=19820015733 (accessed on 1 April 2020).
6. Tucker, C.J. Red and photographic infrared linear combinations for monitoring vegetation. *Remote Sens. Environ.* **1979**, *8*, 127–150. [CrossRef]
7. Tucker, C.J.; Pinzon, J.E.; Brown, M.E.; Slayback, D.A.; Pak, E.W.; Mahoney, R.; Vermote, E.F.; El Saleous, N. An extended AVHRR 8-km NDVI dataset compatible with MODIS and SPOT vegetation NDVI data. *Int. J. Remote Sen.* **2005**, *26*, 4485–4498. [CrossRef]
8. Kogan, F.N. Remote sensing of weather impacts on vegetation in non-homogeneous areas. *Int. J. Remote Sens.* **1990**, *11*, 1405–1419. [CrossRef]
9. Kogan, F.N. Application of vegetation index and brightness temperature for drought detection. *Adv. Space Res.* **1995**, *15*, 91–100. [CrossRef]
10. Kogan, F.N. Droughts of the late 1980s in the United States as derived from NOAA polar-orbiting satellite data. *Bull. Am. Meteorol. Soc.* **1995**, *76*, 655–668. [CrossRef]
11. Quiring, S.M.; Ganesh, S. Evaluating the utility of the Vegetation Condition Index (VCI) for monitoring meteorological drought in Texas. *Agric. For. Meteorol.* **2010**, *150*, 330–339. [CrossRef]
12. Unganai, L.S.; Kogan, F.N. Southern Africa's recent droughts from space. *Adv. Space Res.* **1998**, *21*, 507–511. [CrossRef]
13. Wang, P.X.; Li, X.W.; Gong, J.Y.; Song, C. Vegetation temperature condition index and its application for drought monitoring. In *IGARSS 2001. Scanning the Present and Resolving the Future. Proceedings. IEEE 2001 International Geoscience and Remote Sensing Symposium (Cat. No. 01CH37217)*; IEEE: New York, NY, USA, 2001; Volume 1, pp. 141–143.
14. Bhuiyan, C.; Singh, R.P.; Kogan, F.N. Monitoring drought dynamics in the Aravalli region (India) using different indices based on ground and remote sensing data. *Int. J. Appl. Earth Obs.* **2006**, *8*, 289–302. [CrossRef]
15. Chang, S.; Wu, B.; Yan, N.; Davdai, B.; Nasanbat, E. Suitability assessment of satellite-derived drought indices for Mongolian grassland. *Remote Sens.* **2017**, *9*, 650. [CrossRef]
16. Kogan, F.N. Global drought watch from space. *Bull. Am. Meteorol. Soc.* **1997**, *78*, 621–636. [CrossRef]
17. Svoboda, M.; LeComte, D.; Hayes, M.; Heim, R.; Gleason, K.; Angel, J.; Rippey, B.; Tinker, R.; Palecki, M.; Stooksbury, D.; et al. The drought monitor. *Bull. Am. Meteorol. Soc.* **2002**, *83*, 1181–1190. [CrossRef]
18. Mannava, V.K.S.; Raymond, P.M.; Donald, A.W.; Deborah, A.W. (Eds.) Agricultural Drought Indices. In Proceedings of the WMO/UNISDR Expert Group Meeting on Agricultural Drought Indices, Murcia, Spain, 2–4 June 2010; World Meteorological Organization: Geneva, Switzerland, 2011; p. 197.

19. Lawrimore, J.; Heim, R.R., Jr.; Svoboda, M.; Swail, V.; Englehart, P.J. Beginning a new era of drought monitoring across North America. *Bull. Am. Meteorol. Soc.* **2002**, *83*, 1191–1192. [CrossRef]
20. Heim, R.R., Jr.; Brewer, M.J. The global drought monitor portal: The foundation for a global drought information system. *Earth Interact.* **2012**, *16*, 1–28. [CrossRef]
21. Global Drought Information System. Available online: https://www.drought.gov/gdm/current-conditions (accessed on 3 April 2020).
22. Kogan, F. *Remote Sensing for Food Security*; Springer International Publishing: Berlin/Heidelberg, Germany, 2019.
23. Kogan, F.; Guo, W.; Yang, W.; Harlan, S. Space-based vegetation health for wheat yield modeling and prediction in Australia. *J. Appl. Remote Sens.* **2018**, *12*, 026002.
24. Najafi, E.; Devineni, N.; Khanbilvardi, R.M.; Kogan, F. Understanding the changes in global crop yields through changes in climate and technology. *Earth's Future* **2018**, *6*, 410–427. [CrossRef]
25. Kogan, F.N. Climate constraints and trends in global grain production. *Agric. For. Meteorol.* **1986**, *37*, 89–107. [CrossRef]
26. Kogan, F.; Salazar, L.; Roytman, L. Forecasting crop production using satellite-based vegetation health indices in Kansas, USA. *Int. J. Remote Sens.* **2012**, *33*, 2798–2814. [CrossRef]
27. Salazar, L.; Kogan, F.; Roytman, L. Use of remote sensing data for estimation of winter wheat yield in the United States. *Int. J. Remote Sens.* **2007**, *28*, 3795–3811. [CrossRef]
28. Menzhulin, G.; Shamshurina, N.; Pavlovsky, A.; Kogan, F. New regression models for prediction of grain yield anomalies from satellite-based vegetation health indices. In *Use of Satellite and In-Situ Data to Improve Sustainability*; Springer: Dordrecht, The Netherlands, 2011; pp. 105–112.
29. Salazar, L.; Kogan, F.; Roytman, L. Using vegetation health indices and partial least squares method for estimation of corn yield. *Int. J. Remote Sens.* **2008**, *29*, 175–189. [CrossRef]
30. Kogan, F.; Adamenko, T.; Kulbida, M. Satellite-based crop production monitoring in Ukraine and regional food security. In *Use of Satellite and In-Situ Data to Improve Sustainability*; Springer: Dordrecht, The Netherlands, 2011; pp. 99–104.
31. Kogan, F.; Kussul, N.; Adamenko, T.; Skakun, S.; Kravchenko, O.; Kryvobok, O.; Shelestov, A.; Kolotii, A.; Kussul, O.; Lavrenyuk, A. Winter wheat yield forecasting in Ukraine based on Earth observation, meteorological data and biophysical models. *Int. J. Appl. Earth Obs.* **2013**, *23*, 192–203. [CrossRef]
32. Kogan, F.; Kussul, N.N.; Adamenko, T.I.; Skakun, S.V.; Kravchenko, A.N.; Krivobok, A.A.; Shelestov, A.Y.; Kolotii, A.V.; Kussul, O.M.; Lavrenyuk, A.N. Winter wheat yield forecasting: A comparative analysis of results of regression and biophysical models. *J. Autom. Inform. Sci.* **2013**, *45*, 68–81. [CrossRef]
33. Seiler, R.A.; Kogan, F.; Wei, G. Monitoring weather impact and crop yield from NOAA AVHRR data in Argentina. *Adv. Space Res.* **2000**, *26*, 1177–1185. [CrossRef]
34. Seiler, R.A.; Kogan, F.; Wei, G.; Vinocur, M. Seasonal and interannual responses of the vegetation and production of crops in Cordoba-Argentina assessed by AVHRR derived vegetation indices. *Adv. Space Res.* **2007**, *39*, 88–94. [CrossRef]
35. Seiler, R.A.; Kogan, F. Monitoring ENSO cycles and their impacts on crops in Argentina from NOAA-AVHRR satellite data. *Adv. Space Res.* **2002**, *30*, 2489–2493. [CrossRef]
36. Akhand, K.; Nizamuddin, M.; Roytman, L.; Kogan, F.; Goldberg, M. Using artificial neural network and satellite data to predict rice yield in Bangladesh. In *Remote Sensing and Modeling of Ecosystems for Sustainability XII*; International Society for Optics and Photonics: Bellingham, WA, USA, 2015; Volume 9610, p. 96100E.
37. Nizamuddin, M.; Akhand, K.; Roytman, L.; Kogan, F.; Goldberg, M. Using NOAA/AVHRR based remote sensing data and PCR method for estimation of Aus rice yield in Bangladesh. In *Sensing for Agriculture and Food Quality and Safety VII*; International Society for Optics and Photonics: Bellingham, WA, USA, 2015; Volume 9488, p. 94880O.
38. Rahman, A.; Kaisar, K.; Krakauer, N.Y.; Roytman, L.; Kogan, F. Using AVHRR-Based Vegetation Health Indices for Estimation of Potato Yield in Bangladesh. *J. Civ. Environ. Eng.* **2012**, *2*. [CrossRef]
39. Akhand, K.; Nizamuddin, M.; Roytman, L.; Kogan, F. Using remote sensing satellite data and artificial neural network for prediction of potato yield in Bangladesh. In *Remote Sensing and Modeling of Ecosystems for Sustainability XIII*; International Society for Optics and Photonics: Bellingham, WA, USA, 2016; Volume 9975, p. 997508.

40. Liu, W.T.; Kogan, F. Monitoring Brazilian soybean production using NOAA/AVHRR based vegetation condition indices. *Int. J. Remote Sens.* **2002**, *23*, 1161–1179. [CrossRef]
41. Dabrowska-Zielinska, K.; Kogan, F.; Ciolkosz, A.; Gruszczynska, M.; Kowalik, W. Modelling of crop growth conditions and crop yield in Poland using AVHRR-based indices. *Int. J. Remote Sens.* **2002**, *23*, 1109–1123. [CrossRef]
42. Bokusheva, R.; Kogan, F.; Vitkovskaya, I.; Conradt, S.; Batyrbayeva, M. Satellite-based vegetation health indices as a criteria for insuring against drought-related yield losses. *Agric. For. Meteorol.* **2016**, *220*, 200–206. [CrossRef]
43. Bhuiyan, C.; Saha, A.K.; Bandyopadhyay, N.; Kogan, F.N. Analyzing the impact of thermal stress on vegetation health and agricultural drought—A case study from Gujarat, India. *GISci. Remote Sens.* **2017**, *54*, 678–699. [CrossRef]
44. Kogan, F.; Guo, W.; Strashnaia, A.; Kleshenko, A.; Chub, O.; Virchenko, O. Modelling and prediction of crop losses from NOAA polar-orbiting operational satellites. *Geomat. Nat. Hazards Risk* **2016**, *7*, 886–900. [CrossRef]
45. Kogan, F.; Yang, B.; Guo, W.; Pei, Z.; Jiao, X. Modelling corn production in China using AVHRR-based vegetation health indices. *Int. J. Remote Sens.* **2005**, *26*, 2325–2336. [CrossRef]
46. Unganai, L.S.; Kogan, F.N. Drought monitoring and corn yield estimation in Southern Africa from AVHRR data. *Remote Sens. Environ.* **1998**, *63*, 219–232. [CrossRef]
47. Hochrainer-Stigler, S.; van der Velde, M.; Fritz, S.; Pflug, G. Remote sensing data for managing climate risks: Index-based insurance and growth related applications for smallhold-farmers in Ethiopia. *Clim. Risk Manag.* **2014**, *6*, 27–38. [CrossRef]
48. Wu, D.; Qu, J.J.; Hao, X.; Xiong, J. The 2012 agricultural drought assessment in Nebraska using MODIS satellite data. In *2013 Second International Conference on Agro-Geoinformatics (Agro-Geoinformatics)*; IEEE: New York, NY, USA, 2013; pp. 170–175.
49. Chen, C.F.; Son, N.T.; Chen, C.R.; Chiang, S.H.; Chang, L.Y.; Valdez, M. Drought monitoring in cultivated areas of Central America using multi-temporal MODIS data. *Geomat. Nat. Hazards Risk* **2017**, *8*, 402–417. [CrossRef]
50. Sholihah, R.I.; Trisasongko, B.H.; Shiddiq, D.; La Ode, S.I.; Kusdaryanto, S.; Panuju, D.R. Identification of agricultural drought extent based on vegetation health indices of Landsat data: Case of Subang and Karawang, Indonesia. *Procedia Environ. Sci.* **2016**, *33*, 14–20. [CrossRef]
51. Ghaleb, F.; Mario, M.; Sandra, A.N. Regional landsat-based drought monitoring from 1982 to 2014. *Climate* **2015**, *3*, 563–577. [CrossRef]
52. Tucker, C.J.; Newcomb, W.W.; Dregne, H.E. AVHRR data sets for determination of desert spatial extent. *Int. J. Remote Sens.* **1994**, *15*, 3547–3565. [CrossRef]
53. James, M.E.; Kalluri, S.N. The Pathfinder AVHRR land data set: An improved coarse resolution data set for terrestrial monitoring. *Int. J. Remote Sens.* **1994**, *15*, 3347–3363. [CrossRef]
54. Myneni, R.B.; Keeling, C.D.; Tucker, C.J.; Asrar, G.; Nemani, R.R. Increased plant growth in the northern high latitudes from 1981 to 1991. *Nature* **1997**, *386*, 698–702. [CrossRef]
55. Nemani, R.R.; Keeling, C.D.; Hashimoto, H.; Jolly, W.M.; Piper, S.C.; Tucker, C.J.; Myneni, R.B.; Running, S.W. Climate-driven increases in global terrestrial net primary production from 1982 to 1999. *Science* **2003**, *300*, 1560–1563. [CrossRef] [PubMed]
56. Kogan, F.; Guo, W.; Jelenak, A. Global vegetation health: Long-term data records. In *Use of Satellite and In-Situ Data to Improve Sustainability*; Springer: Dordrecht, The Netherlands, 2011; pp. 247–255.
57. Yang, W.; Guo, W.; Kogan, F. VIIRS-based high resolution spectral vegetation indices for quantitative assessment of vegetation health: Second version. *Int. J. Remote Sens.* **2018**, *39*, 7417–7436. [CrossRef]
58. Joint Polar Satellite System Mission and Instruments. 2011. Available online: http://www.jpss.noaa.gov/mission_and_instruments.html (accessed on 21 April 2020).
59. Kuciauskas, A.; Solbrig, J.; Lee, T.; Hawkins, J.; Miller, S.; Surratt, M.; Richardson, K.; Bankert, R.; Kent, J. Next-generation satellite meteorology technology unveiled. *Bull. Am. Meteorol. Soc.* **2013**, *94*, 1824–1825. [CrossRef]
60. Shao, X.; Cao, C.; Xiong, X.; Liu, T.C.; Zhang, B.; Uprety, S. Orbital variations and impacts on observations from SNPP, NOAA 18-20, and AQUA sun-synchronous satellites. In *Earth Observing Systems XXIII*; International Society for Optics and Photonics: Bellingham, WA, USA, 2018; Volume 10764, p. 107641U.

61. Kogan, F.; Goldberg, M.; Schott, T.; Guo, W. Suomi NPP/VIIRS: Improving drought watch, crop loss prediction, and food security. *Int. J. Remote Sens.* **2015**, *36*, 5373–5383. [CrossRef]
62. Yang, W.; Kogan, F.; Guo, W.; Chen, Y. A novel re-compositing approach to create continuous and consistent cross-sensor/cross-production global NDVI datasets. *Int. J. Remote Sens.* under review.
63. Kogan, F.; Guo, W.; Yang, W. SNPP/VIIRS vegetation health to assess 500 California drought. *Geomat. Nat. Hazards Risk* **2017**, *8*, 1383–1395. [CrossRef]
64. Kogan, F.; Guo, W.; Yang, W. Drought and food security prediction from NOAA new generation of operational satellites. *Geomat. Nat. Hazards Risk* **2019**, *10*, 651–666. [CrossRef]
65. Long, D.; Scanlon, B.R.; Longuevergne, L.; Sun, A.Y.; Fernando, D.N.; Save, H. GRACE satellite monitoring of large depletion in water storage in response to the 2011 drought in Texas. *Geophys. Res. Lett.* **2013**, *40*, 3395–3401. [CrossRef]
66. AghaKouchak, A.; Cheng, L.; Mazdiyasni, O.; Farahmand, A. Global warming and changes in risk of concurrent climate extremes: Insights from the 2014 California drought. *Geophys. Res. Lett.* **2014**, *41*, 8847–8852. [CrossRef]
67. Lesk, C.; Rowhani, P.; Ramankutty, N. Influence of extreme weather disasters on global crop production. *Nature* **2016**, *529*, 84–87. [CrossRef] [PubMed]
68. Dai, A. Increasing drought under global warming in observations and models. *Nat. Clim. Chang.* **2013**, *3*, 52–58. [CrossRef]
69. Sheffield, J.; Wood, E.F.; Roderick, M.L. Little change in global drought over the past 60 years. *Nature* **2012**, *491*, 435–438. [CrossRef] [PubMed]
70. Trenberth, K.E.; Dai, A.; Van Der Schrier, G.; Jones, P.D.; Barichivich, J.; Briffa, K.R.; Sheffield, J. Global warming and changes in drought. *Nat. Clim. Chang.* **2014**, *4*, 17–22. [CrossRef]
71. Kogan, F.; Guo, W.; Yang, W. Near 40-year drought trend during 1981–2019 earth warming and food security. *Geomat. Nat. Hazards Risk* **2020**, *11*, 469–490. [CrossRef]
72. Wang, W.; Zhu, Y.; Xu, R.; Liu, J. Drought severity change in China during 1961–2012 indicated by SPI and SPEI. *Nat. Hazards* **2015**, *75*, 2437–2451. [CrossRef]
73. Chen, C.; Park, T.; Wang, X.; Piao, S.; Xu, B.; Chaturvedi, R.K.; Fuchs, R.; Brovkin, V.; Ciais, P.; Fensholt, R.; et al. China and India lead in greening of the world through land-use management. *Nat. Sustain.* **2019**, *2*, 122–129. [CrossRef]
74. Karnieli, A.; Bayasgalan, M.; Bayarjargal, Y.; Agam, N.; Khudulmur, S.; Tucker, C.J. Comments on the use of the vegetation health index over Mongolia. *Int. J. Remote Sens.* **2006**, *27*, 2017–2024. [CrossRef]
75. Karnieli, A.; Agam, N.; Pinker, R.T.; Anderson, M.; Imhoff, M.L.; Gutman, G.G.; Panov, N.; Goldberg, A. Use of NDVI and land surface temperature for drought assessment: Merits and limitations. *J. Clim.* **2010**, *23*, 618–633. [CrossRef]
76. Bento, V.A.; Gouveia, C.M.; DaCamara, C.C.; Trigo, I.F. A climatological assessment of drought impact on vegetation health index. *Agric. For. Meteorol.* **2018**, *259*, 286–295. [CrossRef]
77. Heeks, R. Information and Communication Technologies, Poverty and Development; 1999. Available online: https://ssrn.com/abstract=3477770 (accessed on 9 November 2019).
78. International Telecommunication Union Technology Watch Report, ICTs and Food Security. 2009. Available online: https://www.itu.int/dms_pub/itu-t/oth/23/01/T230100000B0001PDFE.pdf (accessed on 28 November 2020).
79. Nakasone, E.; Torero, M. A text message away: ICTs as a tool to improve food security. *Agric. Econ.* **2016**, *47*, 49–59. [CrossRef]
80. Latchininsky, A.V. Locusts and remote sensing: A review. *J. Appl. Remote Sens.* **2013**, *7*, 075099. [CrossRef]
81. Cressman, K. Role of remote sensing in desert locust early warning. *J. Appl. Remote Sens.* **2013**, *7*, 075098. [CrossRef]